

Photostability of colloidal single photon emitter in near-infrared regime at room temperature

Si-Yue Jin(靳思玥) and Xing-Sheng Xu(许兴胜)

Citation: Chin. Phys. B, 2024, 33 (**3**): 036102. DOI: 10.1088/1674-1056/ad1090
Journal homepage: http://cpb.iphy.ac.cn; http://iopscience.iop.org/cpb

What follows is a list of articles you may be interested in

Onion-structured transition metal dichalcogenide nanoparticles by laser fabrication in liquids and atmospheres

Le Zhou(周乐), Hongwen Zhang(张洪文), Qian Zhao(赵倩), and Weiping Cai(蔡伟平)
Chin. Phys. B, 2022, 31 (**7**): 076106. DOI: 10.1088/1674-1056/ac539c

Stability and luminescence properties of $CsPbBr_3$/CdSe/Al core-shell quantum dots

Heng Yao(姚恒), Anjiang Lu(陆安江), Zhongchen Bai(白忠臣), Jinguo Jiang(蒋劲国), and Shuijie Qin(秦水介)
Chin. Phys. B, 2022, 31 (**4**): 046106. DOI: 10.1088/1674-1056/ac5978

Characterization, spectroscopic investigation of defects by positron annihilation, and possible application of synthesized PbO nanoparticles

Sk Irsad Ali, Anjan Das, Apoorva Agrawal, Shubharaj Mukherjee, Maudud Ahmed, P M G Nambissan, Samiran Mandal, and Atis Chandra Mandal
Chin. Phys. B, 2021, 30 (**2**): 026103. DOI: 10.1088/1674-1056/abd2a9

Impeding anion exchange to improve composition stability of $CsPbX_3$ (X=Cl, Br) nanocrystals through facilely fabricated Cs_4PbX_6 shell

Zhaohui Shen(申朝晖), Pengjie Song(宋鹏杰), Bo Qiao(乔泊), Jingyue Cao(曹靖玥), Qiongyu Bai(白琼宇), Dandan Song(宋丹丹), Zheng Xu(徐征), Suling Zhao(赵谡玲), Gaoqian Zhang(张高倩), Yuanjun Wu(吴元均)
Chin. Phys. B, 2019, 28 (**8**): 086102. DOI: 10.1088/1674-1056/28/8/086102

Sputtered gold nanoparticles enhanced quantum dot light-emitting diodes

Abida Perveen, Xin Zhang(张欣), Jia-Lun Tang(汤加仑), Deng-Bao Han(韩登宝), Shuai Chang(常帅), Luo-Gen Deng(邓罗根), Wen-Yu Ji(纪文宇), Hai-Zheng Zhong(钟海政)
Chin. Phys. B, 2018, 27 (**8**): 086101. DOI: 10.1088/1674-1056/27/8/086101

Photostability of colloidal single photon emitter in near-infrared regime at room temperature

Si-Yue Jin(靳思玥)[1,2] and Xing-Sheng Xu(许兴胜)[1,2,3,†]

[1] *Key Laboratory of Optoelectronic Materials and Devices, Chinese Academy of Sciences, Beijing* 100083, *China*
[2] *Center of Materials Science and Optoelectronics Engineering, University of Chinese Academy of Sciences, Beijing* 100049, *China*
[3] *Hefei National Laboratory, Hefei* 230088, *China*

(Received 14 August 2023; revised manuscript received 19 October 2023; accepted manuscript online 29 November 2023)

The photostability of a colloidal single photon emitter in near-infrared regime at room temperature is investigated. The fluorescence lifetime, blinking phenomenon, and anti-bunching effect of a single CdTeSe/ZnS quantum dot with an emission wavelength of 800 nm at room temperature are studied. The second-order correlation function at zero delay time is much smaller than 0.1, which proves that the emission from single quantum dots at 800 nm is a highly pure single-photon source. The effects of the irradiation duration on the fluorescence from single quantum dots are analyzed. The experimental results can be explained by a recombination model including a multi-nonradiative recombination center model and a multi-charged model.

Keywords: colloidal quantum dots, single photon source, blinking

PACS: 61.46.Df, 61.46.Hk, 78.55.–m **DOI:** 10.1088/1674-1056/ad1090

1. Introduction

In recent years, breakthroughs in single-photon source (SPS) technology have received much attention. The SPS technology has been applied to quantum communication, quantum computing, quantum key distribution (QKD), and other quantum information fields.[1] Quantum dots (QDs) have also been widely studied as important materials for making single-photon quantum light sources. Arakawa and Sakaki first proposed the concept of QDs in 1982.[2] At present, two methods, i.e., epitaxy method and wet chemical method, are mainly used to produce QDs . Both methods can efficiently fabricate a single QD, while core–shell colloidal quantum dots (CQDs) based on II–VI compounds can emit single photons at room temperature due to their unique electronic properties.[3,4] Herein we use core–shell CQDs as single-photon emitters in this experiment because of their room temperature operability and many other advantages. In 2000, CQDs were first demonstrated as SPSs by Michler, *et al*.[3] In 2004, Brokmann *et al*. successfully made an SPS by using CdSe/ZnS CQDs with a central wavelength of 560 nm, the CQDs showed obvious anti-bunching effect, and the effect of Auger recombination on luminescence of CQDs SPS was discussed.[5] In 2009, Yuan *et al*. studied the anti-bunching and blinking of CdSe/ZnS CQDs at a wavelength of 700 nm, by coupling a single QD with a silver nano-prism, they suppressed the blinking phenomenon and enhanced single-photon emission.[6] We developed and reported CQDs at a wavelength of 650 nm as an SPS at room temperature in 2010.[7] Tang *et al*. developed all-inorganic $CsPbX_3$ QDs with an adjustable photoluminescence wavelength (400 nm–700 nm) by adjusting the different compositions.[8] In 2017, Chandrasekaran *et al*. investigated the feasibility of colloidal core/shell InP/ZnSe CQDs as an SPS.[9] In order to transfer the maximum emission wavelength to infrared (IR) or near infrared (NIR), the third element such as Te can be added into the core layer of CdSe. In recent years, some studies have reported the synthesis methods and optical properties of $CdTe_xSe_{1-x}$-based IR/NIR light-emitting CQDs.[10,11] In 2017, Hung *et al*. synthesized CdTeSe CQDs at a temperature of 260 °C and realized the single-photon emission of individual single-core/shell CdTeSe/ZnSe CQDs.[12]

However, until now, an SPS of CdTeSe/ZnSe CQDs with a wavelength of 800 nm at room temperature has rarely been reported.[13] The QDs with longer luminous wavelengths are sensitive to defect and surface state. These defects and surface state can reduce the efficiency of radiation recombination of electron and holes, generating non-radiation recombination, thus reducing the fluorescence efficiency. The size of the quantum dot with longer luminous wavelength is larger, and the dimension of size and structure can also cause the fluorescence efficiency to decrease. This may generate a variety of energy levels in QDs, thus complicating the radiation recombination of electrons and holes. Due to the lower quantum efficiency of CQDs at longer wavelength, the single photon emission around 800 nm is relatively difficult to realize. In order to improve the fluorescence efficiency of long wavelength QDs, we set up a precise measurement system in the experiment. In this work, a single 800-nm CQD on a dielectric material is investigated for SPS, and the fluorescence lifetime,

†Corresponding author. E-mail: xsxu@semi.ac.cn

© 2024 Chinese Physical Society and IOP Publishing Ltd

blinking, and anti-bunching phenomena of a single 800-nm CQD are characterized. A second-order correlation function of $g^2(0) \approx 0.005$ is obtained, proving that the emission from single CQD at 800 nm is a high-quality SPS. The optical properties of the single CQD SPS at 800 nm under various irradiation durations are studied, and the photostability of colloidal single-photon emitters under near-infrared conditions at room temperature is investigated. The emission wavelength of the investigated single photon source is about 800 nm, which is comparable to the wavelength of the practical QKD application system, such as Micius, quantum communication satellite system. Combined with room-temperature working condition, the single photon source at 800 nm has important potential application prospects.

2. Materials and experiment system

Qdot^{TM} 800 ITK^{TM} CQDs from Thermo Fisher were used in our experiment.[14] The structural schematic diagram of a colloidal quantum dot is shown in Fig. 1(a). The thickness of the core–shell layer was a few nanometers, but with the surface polymer, the total diameter of the quantum dots reached 15 nm–20 nm. The emission wavelength of the QDs we used was 795 nm±10 nm, the FWHM was 89 nm, and the quantum yield was 63%.[14] The photoluminescence (PL) spectrum of CQDs in solution was measured, the actual center emission wavelength was 780 nm as shown in Fig. 1(b). The images of CQDs scanned by using Oxford's AFM instrument are shown in Figs. 1(c) and 1(d). The original concentration of CQDs was 10^{-6} M and diluted to 5×10^{-11} M with hexane (C_6H_{14}) for characterizing single photon emission. We introduced the low-concentration CQDs onto the surface of a piece of sapphire material with a thickness of 175 μm by using a drop-dragging method.[15]

The schematic diagram of measuring optical path in the experiment is shown in Fig. 2(a). To improve the collection efficiency of the single-photon signals, an oil objective with refractive index matching oil was used as shown in Fig. 2(b); the oil objective lens was 100× with N.A. = 1.25. The CQDs were excited by a 400-nm laser with a pulse width of 30 ps and a repetition rate of 10 MHz. The laser passed through an attenuator, a small aperture and the oil immersion objective and focused on a single CQD. The photons emitted from the CQDs were collected by the same objective lens. The collected photons passed through a reflector and a 700-nm long pass filter, and then they were sent to a standard Hanbury–Brown and Twiss (HBT) system for characterization. The single-photon signal was detected by two silicon avalanche photodiodes (Si-APDs).

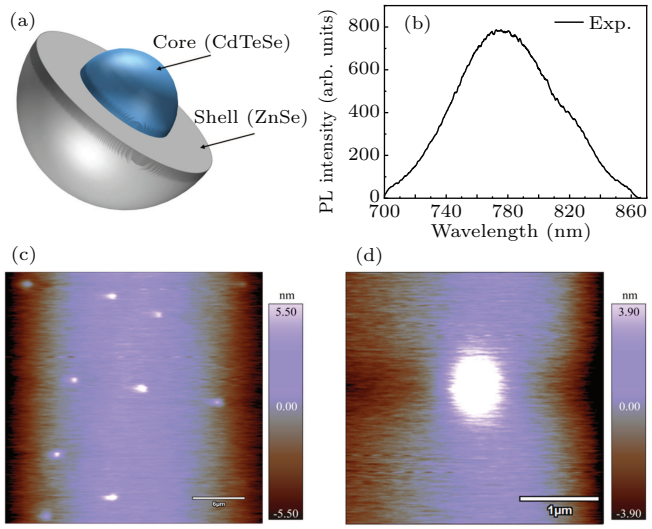


Fig. 1. (a) Structural schematic diagram of CQD. (b) PL spectrum of CQDs in hexane solution. (c) Images of multiple 800-nm CQDs and (d) single 800-nm CQDs on a sapphire substrate scanned by Oxford's AFM instrument.

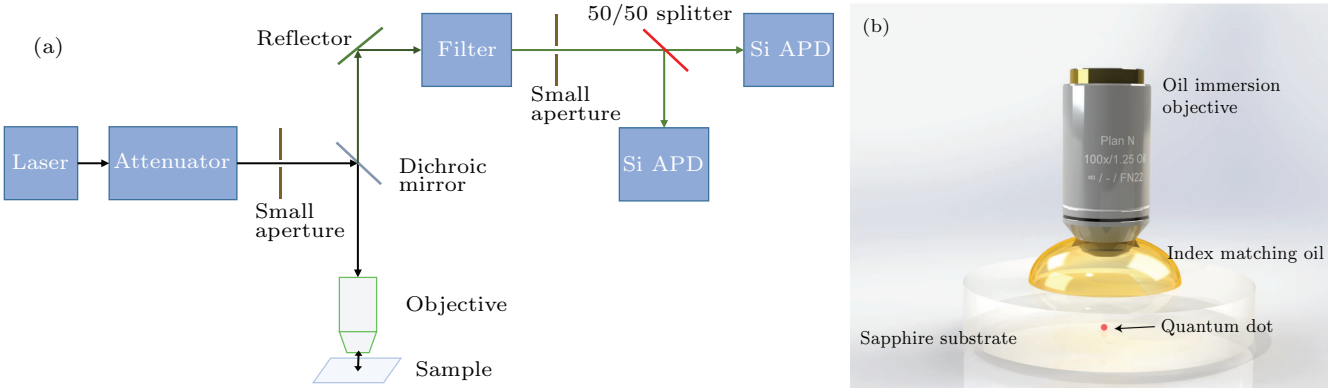


Fig. 2. (a) Schematic diagram of measuring optical path in the experiment. (b) Experimental excitation arrangement.

3. Antibunching effect with different irradiation time

The coincidence counts changing with delay time are measured from a single CQD for different irradiation durations under the same conditions at room temperature, and the results are shown in Fig. 3. The excitation power transmitted through the objective lens was 0.028 mW. The coincidence counts as a function of delay time for different irradiation time are shown

in Figs. 3(a)–3(f), and the collection time is 12 min, 24 min, 48 min, 60 min, 84 min, and 108 min, respectively. The coincidence counts gradually increase, and the coincidence peak at the zero point of the delay time gradually increases in the coincidence–count curves from Figs. 3(a)–3(f) as the collection time increases. As shown in Figs. 3(a)–3(d), when the collection time is less than 60 min, the coincidence–count curve near the zero point of the delay time is relatively smooth, and there is a large and deep dip due to antibunching effect of single photon emission from the single CQD. In Figs. 3(e)–3(f), when the collection time is longer than 60 min, a small peak gradually appears in the dip, which becomes more obvious in Fig. 3(f) with a collection time of 108 min. The background, due to the dark counts of the Si-APDs and the effect of the measurement system, was subtracted in Figs. 3(a)–3(f). The coincidence–count curves in Figs. 3(a)–3(f) were fitted to a multi-exponential function as follows:

$$y = y_0 + \sum_{i=0}^{4} A_i \times \exp(-|(x - x_i - T \times i)/t_i|), \qquad (1)$$

where A_0, A_1, A_2, A_3, and A_4 are amplitudes of the five coincidence peaks in the anti-bunching curve, and T is the time period between the coincidence peaks.

After fitting with Eq. (1), the obtained amplitudes A_0, A_1, A_2, and A_4 were added and averaged and then divided by A_3 to calculate the second-order correlation function, where A_3 corresponds to the amplitude at the zero point of the delay time. Considering the standard deviation, the calculated second-order correlation functions at the zero point of the delay time in Figs. 3(a)–3(d) are $g^2_{\rm a}(0) \approx 0.022 \pm 0.0012$, $g^2_{\rm b}(0) \approx 0.005 \pm 0.0004$, $g^2_{\rm c}(0) \approx 0.026 \pm 0.0012$, $g^2_{\rm d}(0) \approx 0.048 \pm 0.0009$, respectively. The experimental curves of the coincidence counts accord well with the fitting curves (Eq. (1)), and both the experimental curves and fitting curves near the zero point of the delay time are flat and smooth. All the values of the second-order correlation functions at the zero point of the delay time in Figs. 3(a)–3(d) are less than 0.05 for those irradiation durations. In Fig. 3(e) irradiation time is 84 min and $g^2_{\rm e}(0) \approx 0.104 \pm 0.0017$, and in Fig. 3(f) the irradiation time is 108 min, and $g^2_{\rm f}(0) \approx 0.203 \pm 0.0020$. A small peak appears at the zero point of the delay time, and the values of the second-order correlation functions at the zero point of the delay time reach to 0.104 and 0.203, respectively.

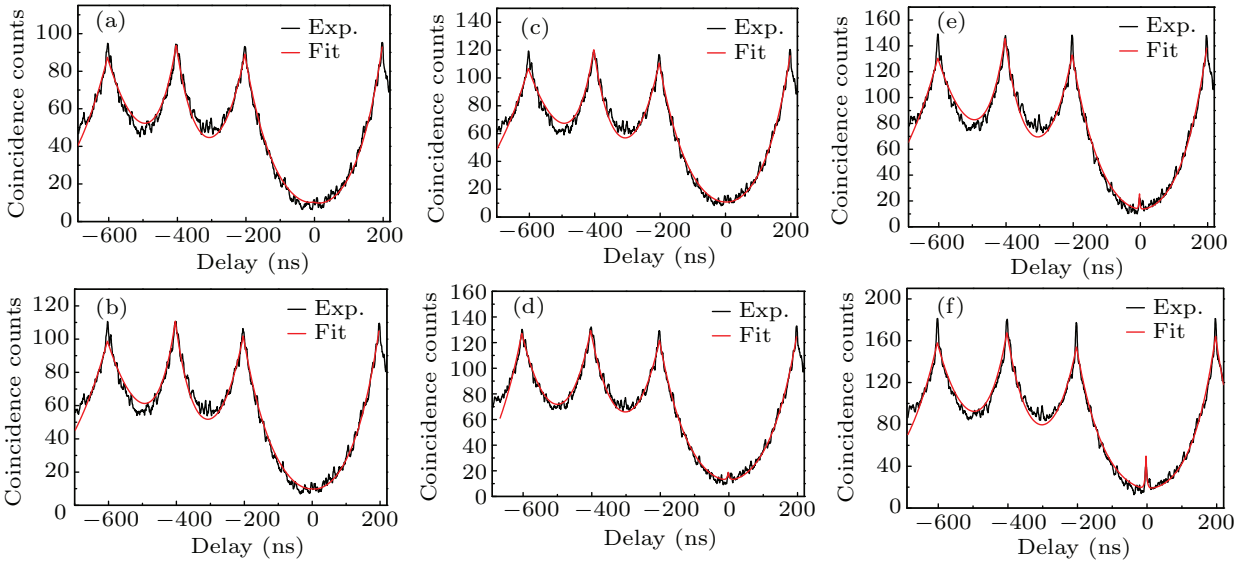


Fig. 3. Coincidence counts as a function of the delay time for irradiation duration of (a) 12 min, (b) 24 min, (c) 48 min, (d) 60 min, (e) 84 min, and (f) 108 min. The anti-bunching was measured continuously for 108 min, and each coincidence curve was collected during the measurement. The black lines denote the experimental results, the red solid lines are fitted by a multi-exponential function, and the solid yellow lines are fitted by an exponential decay function.

The coincidence count rate is defined as the ratio of coincidence count to collection time. The coincidence count rate (black triangles) and the value of the second-order correlation function at the zero point of the delay time (red squares) are compared in Fig. 4. The coincidence count rate decreases as the irradiation time increases, while the value of $g^2(0)$ increases with irradiation time increasing but not linearly; the value of $g^2(0)$ obtained from Fig. 3(b) is smaller than that from Fig. 3(a). The signal collection time in Fig. 3(a) is short and the calculated value of $g^2(0)$ was affected by the background noise. In the case of shorter signal collection time and less accumulation, the adverse effect of background noise on the purity of single photons will be more obvious. Therefore, in Fig. 3(b), under the appropriate acquisition time (24 minutes), the background noise was relatively low, and the obtained minimum value of $g^2(0)$ is about 0.005±0.0004.

We can use the theory of biexcitons proposed by Nair *et al.*[16] to explain our experimental results in Figs. 3 and 4.

They proposed that in anti-bunching effect curves, the appearance of a peak at zero delay time reflects the possibility of generating biexcitons and subsequently generating two photons, while the side peaks result from the emission of excitons and charged excitons. In our experiment, the intensity of the peak at zero delay time increases and the value of $g^2(0)$ increases with irradiation time increasing from Fig. 3(a) to Fig. 3(f), the photostability of colloidal single-photon emitters with a wavelength of 800 nm at room temperature was influenced by the irradiation time. In this process, firstly, long laser irradiation time would reduce the luminous efficiency of CQDs and make the excitons in the CQDs to be charged. The charged excitons are likely to be related to surface trapping, and then non-radiative recombination rate increased, which would make Auger recombination increase and the photobleaching effect would be more serious. Therefore, due to the decrease in exciton yield, the ratio of the corresponding biexciton yield increases, which leads to a decrease in the coincidence count rate and cause the peak at zero delay time. From Figs. 3 and 4, under the same conditions, the limited time that will change the optical property of the single CQDs should be about 80 minutes.

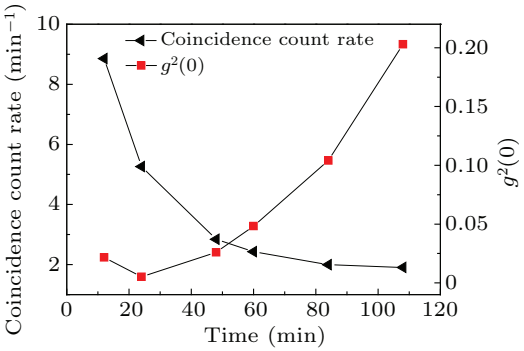


Fig. 4. Coincidence count rate (black triangles) and value of $g^2(0)$ (red squares) versus time in Fig. 3.

4. Photoluminescence blinking of single colloidal quantum dots

Before and after measuring the anti-bunching effect of a single CQD, the measured fluorescence decay curves are respectively denoted as Exp. 1 line and Exp. 2 line in Fig. 5(a). The fluorescence lifetime curves in Fig. 5(a) were fitted to a bi-exponential function. For the lifetime before measuring the anti-bunching effect, the lifetime of the fast process is 0.897 ns, and the lifetime of the slow process is 62.643 ns. The amplitude proportion $M_1/(M_1+M_2)$ of the fast fluorescence lifetime process in the fitting results is 82.70%, and the amplitude proportion of the slow process $M_2/(M_1+M_2)$ is 17.30%. After two-hour measurement of the anti-bunching effect, the lifetime of the fast process is 0.851 ns, and the lifetime of the slow process is 32.489 ns. The amplitude proportion $M_1/(M_1+M_2)$ of the fast fluorescence lifetime process in the fitting results is 98.49%, and the amplitude proportion of the slow process $M_2/(M_1+M_2)$ is 1.51% for line Exp. 2 in Fig. 5(a). It is believed that the charged-exciton emission and multiexciton emission contribute to the fast process of the decay curve.[17] After laser irradiation for a period of time, the fluorescence lifetime of the CQD decreases and the proportion of the fast process increases, indicating an increase in the charged-exciton emission and multi-exciton emission and a decrease in the exciton emission. Biexciton or multiexciton generation would shorten the fluorescence lifetime, and a change in the fluorescence lifetime also confirmed the value of the second-order correlation function at zero delay time changing with irradiation time.

In order to understand the change of lifetime, we investigate the corresponding probability distribution before and after long irradiation time, and the results are shown in Fig. 5(b). We measured the photoluminescence blinking of the CQD before and after measuring the anti-bunching effects. The results are shown in Figs. 5(c) and 5(d), where the vertical axis in the figure represents the photon count rate. The maximum single-photon count rate reaches to 2.5×10^4 cps in Fig. 5(c), while it is 2.0×10^4 cps in Fig. 5(d). Researchers have proved that the probability distribution of the "off-state" of blinking of CQD will not be affected by the environment.[18] The "off-state" probability distribution can be fitted by $P(\tau_{\rm off}) = A\tau_{\rm off}^{-m}$.[19] However, the probability distribution of the "on-state" will be affected by the excitation power[20] and the excitation wavelength.[21] Here, we explored the effect of irradiation time of excitation light on the probability distribution of the "on-state" of the photoluminescence of the CQD. We calculated the probability distribution of the "on-state" from the following formula:

$$P(\tau_{\rm on}) = A\tau_{\rm on}^{-m}\exp(-\tau_{\rm on}/\tau_{\rm fall-off}). \tag{2}$$

This formula was proposed by Peterson and Nesbitt in 2009, and it means that the 1/e time constant $\tau_{\rm fall-off}$ corresponds roughly to the "knee" in the "on-state" distribution.[19] Time constant $\tau_{\rm fall-off}$ is related to the exciton emission efficiency, and the smaller the value of $\tau_{\rm fall-off}$, the larger the proportion of the multi-exciton emission is. By using Eq. (2), the fitting curves are shown in Fig. 5(b) on a log–log scale, and there is a falloff in the power law behavior, corresponding to the time constant in the formula. Before and after the anti-bunching effect measurement, the fitted value of $\tau_{\rm fall-off}$ decreases from 0.25 (red line) to 0.21 (black line), suggesting the occurrence of multi-exciton emission. This result is consistent with the analysis of the anti-bunching effect and fluorescence lifetime.

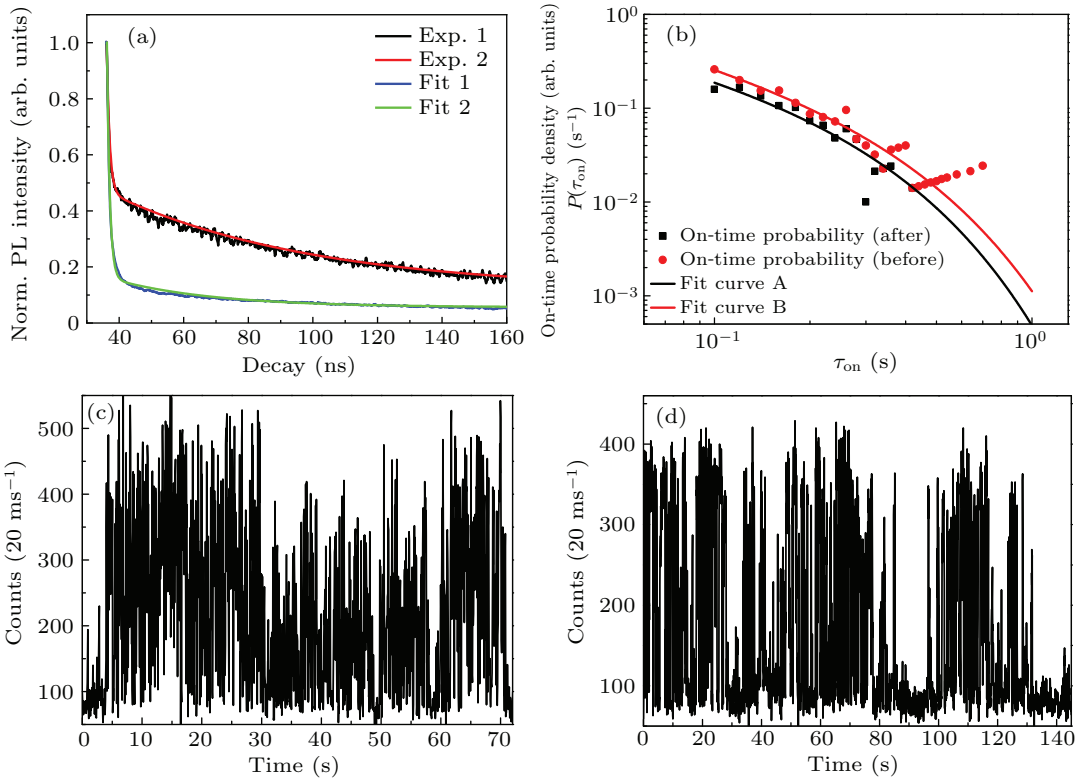


Fig. 5. (a) Fluorescence lifetime of CQD before measuring the anti-bunching effect (Exp. 1), fluorescence lifetime of CQD after measuring the anti-bunching effect (Exp. 2). The curves were normalized (Norm.) and fitted to bi-exponential function (Fit 1 and Fit 2). (b) Probability distribution of the "on-time" before (red) and after (black) the anti-bunching effect measurement. (c) Blinking of the CQD before measuring the anti-bunching effect. (d) Blinking of the CQD after measuring the anti-bunching effect.

Several models have been proposed to explain the blinking phenomenon of the photoluminescence of single CQDs. Zhao *et al*. proposed a model[22] including a trap-assisted process and Auger recombination by combining the multiple nonradiative recombination centers (NRCs) model and multi-charged model.[23] According to this model, in a CQD with a larger "on" fraction in blinking, the number of NRCs decreases or the proximity to the NRC or surface capture sites is limited, and the excitons are more likely to be radiatively recombined. In CQDs with a low "on" fraction, the excitons are more likely to be charged, and carriers are more likely to be acquired by NRCs or surface capture sites, where the carriers are more likely to be nonradiatively recombined. In our experiment, due to long-time irradiation, there is strong carrier trapping, which leads to an increase of the fraction of off-state,[24] the longer the laser irradiation on the CQDs, the lower the "on" fraction is. When a threshold of 150 counts/20 ms is selected, the calculated "on" fraction is 0.62 in Fig. 5(c) and 0.37 in Fig. 5(d). With measurement time (i.e. the irradiation time) increasing, the "on" fraction decreases, and the maintaining time of the "off-state" of the blinking of the CQDs is significantly lengthened to ten seconds or even longer in Fig. 5(d) than in Fig. 5(c). This is because the long-term laser irradiation enhances the Auger recombination rate and leads to high nonradiative recombination rate in the NRCs in the CQDs, the carriers are more likely to be trapped by NRCs or surface capture sites, and the CQDs are more likely to be charged.

By measuring and analyzing the value of the second-order correlation function at zero delay time $g^2(0)$, the fluorescence lifetimes and the blinking phenomena of a single CQD under different irradiation durations, we find that the irradiation time has a great influence on the photostability of colloidal single-photon emitters with a wavelength of 800 nm in the near infrared at room temperature. As the irradiation time increases, the value of $g^2(0)$ increases, the fluorescence lifetime becomes shorter, the intensity of the PL blinking becomes weaker, and the "on" fraction of blinking decreases. This is because of the charged-exciton emission and the occurrence of biexciton or multiexciton emission in the CQDs, these will increase the Auger recombination rate and reduce the exciton recombination rate, resulting in a decreases in the single photon yield of CQDs. We measured some other single CQDs under the similar conditions and obtained similar results. Moreover, we have also studied single-photon emission from an 800-nm CQD for different laser powers.[25] The blinking phenomenon of photoluminescence of the single CQDs brings challenges to their applications, but the blinking can be suppressed. Useful methods such as enhancing the thickness of the shell,[26] changing the structure of shell,[27] using electric field to control the charge transfer of the surrounding environment of CQDs.[28,29] Attaching CQDs to the surfaces of different materials or doping the substrate with metal elements can also control the fluo-

rescence radiation characteristics of the CQDs.[30] We found in experiments that the blinking of CQDs on different materials' surfaces (such as metals, semiconductors, and insulating materials) is different. The photoluminescence blinking from single CQDs on SiO_2, SiN/Si, ITO, and Ti/Au are compared in Fig. 6. It can be found that the occurrence probability of the "on-time" of blinking from single CQDs on ITO or Ti/Au is higher than on SiO_2 and SiN/Si. The method for suppression of blinking of CQDs will be further investigated.

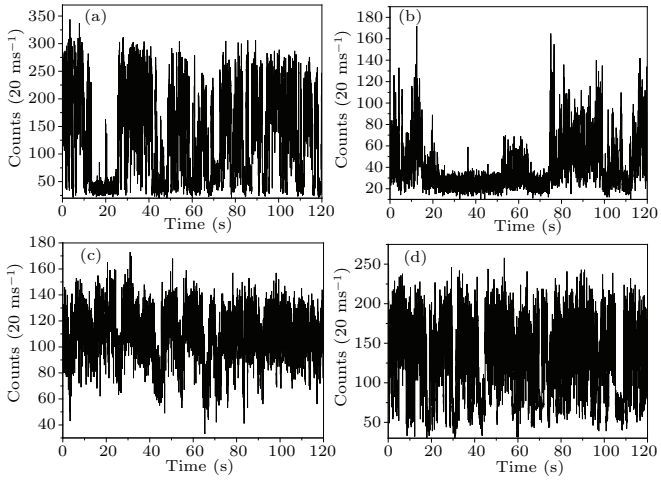


Fig. 6. Photoluminescence blinking from single CQDs on (a) 3-μm SiO_2, (b) SiN/Si, (c) ITO, and (d) Ti/Au.

5. Conclusions

In this work, we have studied the photostability of colloidal single-photon emitters with a wavelength of 800 nm in the near infrared at room temperature, and we obtain a second-order correlation function at zero delay time of $g^2(0) \approx 0.005$, proving that the single CQD at a wavelength of 800 nm is a pure, high-quality SPS. We measure the fluorescence lifetimes, blinking, and anti-bunching effects of single CQDs under different irradiation time. The effect of laser irradiation time on the optical properties of the single CQDs is investigated, which is analyzed by using multiple NRCs and multicharged models. This result has important significance for the future development of near-infrared CQD SPS research. Single photon source based on 800-nm CQDs can be used in a variety of technical fields such as quantum communication systems, quantum computing, high-sensitive quantum sensor, quantum imaging technology, and quantum information processing.

Acknowledgements

Project supported by the National Natural Science Foundation of China (Grant No. 92165202), the Innovation Program for Quantum Science and Technology, China (Grant No. 2021ZD0300701), and the Strategic Priority Research Program (A) of Chinese Academy of Sciences (Grant No. XDA18040300).

References

[1] Gisin N, Ribordy G, Tittel W and Zbinden H 2001 *Rev. Mod. Phys.* **74** 145
[2] Arakawa Y and Sakaki H 1982 *Appl. Phy. Lett.* **40** 939
[3] Michler P, Imamoğlu A, Mason M D, Carson P J, Strouse G F and Buratto S K 2000 *Nature* **406** 968
[4] Lounis B and Moerner W E 2000 *Nature* **407** 491
[5] Brokmann X, Coolen L, Dahan M and Hermier J P 2004 *Phy. Rev. Lett.* **93** 107403
[6] Yuan C T, Yu P, Ko H C, Huang J and Tang J 2009 *ACS Nano* **3** 3051
[7] Xu X, Chen S and Yamada T 2010 *Sci. China. Ser. G* **53** 1619
[8] Tang X S, Hu Z P, Chen W W, Xing X, Hu W, Qiu J, Zang Z G, Du J, Jiang X F and Mai L Q 2016 *Nano Energy* **28** 462
[9] Chandrasekaran V, Tessier M D, Dupont D, Geiregat P, Hens Z and Brainis E 2017 *Nano Lett.* **17** 6104
[10] Ma Q, Yue H, Zhu Y, Wang J, Che Q, Shi R and Yang P 2017 *J. Nanosci. Nanotechnol.* **15** 4442
[11] Liao L, Zhang H and Zhong X 2011 *Journal of Luminescence* **131** 322
[12] Hung L X, Bassène, Pascal D, Thang P N, Loan N T, Willy D D M and Dhawan A R 2017 *RSC Adv.* **7** 47966
[13] Groß H, Hamm J M, Tufarelli T, Hess O and Hecht B 2018 *Sci. Adv.* **4** eaar4906
[14] https://www.thermofisher.com, qdot-nanocrystal-technology
[15] Xu X, Yamada T and Otomo 2009 *Appl. Phys. B* **94** 577
[16] Nair G, Zhao J and Bawendi M G 2011 *Nano Lett.* **11** 1136
[17] Xu X and Li X Y 2015 *Sci. Rep.* **5** 9760
[18] Tang J and Marcus R A 2005 *J. Chem. Phys.* **123** 054704
[19] Peterson J J and Nesbitt D J 2009 *Nano Lett.* **9** 338
[20] Knappenberger K L, Wong D B, Romanyuk Y E and Leone S R 2007 *Nano Lett.* **7** 3869
[21] Kenichi G, Yamada T and Otomo A 2009 *J. Chem. Phys. C* **113** 20161
[22] Zhao J, Chen O, Strasfeld D B and Bawendi M G 2012 *Nano Lett.* **12** 4477
[23] Frantsuzov P A, Volkán-Kacsó S and Jankó B 2009 *Phys. Rev. Lett.* 103, 207402
[24] Califano M 2011 *J. Phys. Chem. C* **115** 18051
[25] Jin S Y and Xu X S 2022 *Europhys. Lett.* **137** 26005
[26] Mahler B, Spinicelli P, Buil S, Quelin X, Hermier J P and Dubertret B 2008 *Nat. Mater.* **7** 659
[27] Chen Y, Vela J, Htoon H, Casson J L, Werder D J and Bussian D A 2008 *J. Am. Chem. Soc.* **130** 5026
[28] Nagao Y, Fujiwara H and Sasaki K 2014 *J. Phys. Chem. C* **118** 20571
[29] LeBlanc S J, McClanahan M R, Moyer T, Jones M and Moyer P J 2014 *Appl. Phys.* **115** 034306
[30] Jin S Y, Song N H and Lian T Q 2010 *ACS Nano* **4** 1545